Original

Liu, J.; Harms, H.; Haramus, V.M.; Mueller-Goymann, C.C.:

Reentrant structural phase transition in amphiphilic self-assembly

In: Soft Matter (2013) Royal Society of Chemistry

DOI: 10.1039/C3SM51239H

Soft Matter

RSC Publishing

COMMUNICATION

View Article Online
View Journal | View Issue

Reentrant structural phase transition in amphiphilic self-assembly†

Cite this: *Soft Matter*, 2013, **9**, 6371

Received 3rd May 2013
Accepted 20th May 2013

DOI: 10.1039/c3sm51239h

www.rsc.org/softmatter

Jianing Liu,*[a] Meike Harms,[a] Vasil M. Garamus[b] and Christel C. Müller-Goymann*[a]

Amphiphilic molecules can self-assemble into a variety of aggregates and mesophases. Yet, predictions of phase transitions are not always met. In this communication, we demonstrate a novel structural phase transition of amphiphilic molecules, quillaja saponin/cholesterol, and discuss the relevance of precursors for forming hierarchical structures. In contrast to the standard sphero-cylinder model, we highlight a three-stage dynamic process of reentrant phase transition induced by cholesterol. It is expected that the obtained results would be helpful to rationalize the rich phase behavior exhibited by surfactant–cosurfactant systems, and to engineer complex nanoarchitectures with tunable size and shape and well-defined biological functions.

Phase transitions of colloids are ubiquitous in nature and have been studied for decades. However, the predictions of phase transitions are not always met.[1] More unusual is the reentrant phase transition, which usually results from a subtle interplay between long-range and short-range interactions as well as entropic contributions, and strongly depends on the balance of the microscopic forces between the particles. Therefore, controlling interparticle interactions, aggregation and the resulting phase behavior in general, and inducing and tuning reentrant phase transition in particular, is not only an important fundamental but also a technological issue. Of particular interest in colloidal suspensions is the phase transition in self-assembly of amphiphilic molecules. This is due in part to their unique physicochemical characteristics and potential applications in nanotechnology, experimental medicine and pharmaceutical science on the one hand, and to the fact that the theoretical understanding of dynamics of phase transitions on the other hand is relatively limited, as amphiphilic molecules in solution present a more complicated case. Although the standard sphero-cylinder model – from a small spherical micelle to an elongated cylindrical midsection capped by two approximately hemi-spherical micellar caps[2] – is widely shared by a number of investigations, two substantive issues remain: (1) in most of these approaches, the rod is usually assumed to be perfectly rigid, without considering high order effects of hierarchy; (2) neither simulation nor experiment shows reentrant phase transition of amphiphilic assembly with non-rigid hierarchical structures in solution, no matter which way is used, by increasing the surfactant concentration or taking into account the effects of foreign cosurfactants. In the wake of spinodal decomposition theory suggested by Flory[3] and Huggins,[4] it would be expected that, by properly blending two different amphiphilic molecules, inducing and tuning reentrant phase transition in solution is sufficiently accessible.

From this perspective, we report a novel structural phase transition in amphiphilic self-assembly of a surfactant quillaja saponin (Quil A) mediated by a cosurfactant, cholesterol (Chol). By a synergetic analysis of small angle X-ray scattering (SAXS) and small angle neutron scattering (SANS) data in both reciprocal- and real-space, we highlight a three-stage dynamic reentrant phase transition in the Quil A/Chol system.

In the system, Quil A, a particular subgroup of amphiphilic molecules, consists of various sugar groups linked by a glycosidic bond to a hydrophobic triterpene ring, and is chosen to build micelles, due to its pharmaceutical potential as an efficient adjuvant,[5] for example, in vaccines against cancer[6] or viral infections.[7] Chol as an essential component (10–50 mol%) of biological membranes, by varying its concentration ratio α, is used to induce and tune structural phase transitions and the resulting hierarchy of Quil A/Chol in virtue of its local organization – ordering, condensing and phase separation – at both low and high concentration,[8,9] as well as its unusual flip-flop motion that maintains the asymmetric distribution.[10,11]

[a]*Institut für Pharmazeutische Technologie, Technische Universität Braunschweig, Mendelssohnstr. 1, D-38106 Braunschweig, Germany. E-mail: jianing.liu@tu-braunschweig.de; c.mueller-goymann@tu-bs.de; Fax: +49-531-3918108; Tel: +49-531-3915710*

[b]*Helmholtz-Zentrum Geesthacht, Zentrum für Materie- und Kürstenforschung, Max-Planck-str. 1, D-21502 Geesthacht, Germany*

† Electronic supplementary information (ESI) available: Material, preparation of Quil A/Chol solution, small-angle X-ray and small-angle neutron scattering measurements. See DOI: 10.1039/c3sm51239h

Using SAXS and SANS, we first investigate structural phase behavior and morphology of Quil A/Chol at different α values in reciprocal space. Fig. 1a presents the SAXS and SANS scattering intensities $I(q)$ at scattering vector q, respectively. A difference between two scattering curves actually reflects their different sensitivities to the electrostatic interactions,[12] hydrogen isotopes[13] and smear effect.[14] Commonly, X-rays as electromagnetic waves interact with electrons. Therefore, the spatial variation of electron density has a stronger impact on the SAXS experiment. Comparatively, neutrons essentially interact only with atomic nuclei, SANS is then sensitive to the isotope effect, and so the structural information provided by SANS is often thought to be more similar or closer to the real sample morphology than SAXS.[13,15]

Fig. 1b displays two very different scattering profiles of $I(q)$, this points out, as described by the Derjaguin–Landau–Verwey–Overbeek (DLVO) theory, that Quil A/Chol systems with an increase in α undergo an interplay between a long-range repulsion arising from the surface charges of the glucuronic acid of Quil A[16] and the surrounding counterions, and a short-range attraction induced by a Chol-mediated "depletion effect" – reduced hydration forces and increased hydrophobic forces[17] – not just in the way that part of Quil A molecules in the system are locally replaced by Chol, resulting in a loss of the charged groups on the sugar chains of Quil A, but also because parts of Chol molecules attach themselves to the Quil A surface, making the surface less charged and more hydrophobic. In line with that, at a very low α (<5%), the $I(q)$ shows a flat forward scattering intensity, the systems are characterized by weakly screened long-range repulsion, which does not allow Quil A/Chol systems to come close to each other, leading to the formation of small equilibrium associates. Whereas, when $\alpha \geq 5\%$, an upward movement of the $I(q)$ at small q clearly embodies that the short-range attractions are dominant[18] due to the stronger depletion effects, and hence, bring the systems into elongated associates. Apparently, such a shift in the balance between the repulsions and attractions means that the spatial variations of electron density in the formation of equilibrium associates are quite different. The same scenario is portrayed in the Holtzer plots $q \times I(q)$ (Fig. 1c). In the small q region, $q \times I(q)$ always bends downwards when $\alpha < 5\%$, and first downwards and then mostly upwards at $q \sim 0.3$ nm^{-1} when $\alpha \geq 5\%$. This situation, indeed, implies that the Quil A/Chol system evolves from a single phase of small associates at lower α into a biphasic system of elongated associates at higher α, that is precisely the way suggested by the standard sphero-cylinder model.

As it turns out, the $I(q)$ and the Holtzer plots also lead to another observation that is of considerable relevance to reentrant phase transition. It can be shown that $q \times I(q)$, when α lies between 12.5% and 20%, features an unstable phase, which separates two metastable nucleation regions. Particularly when

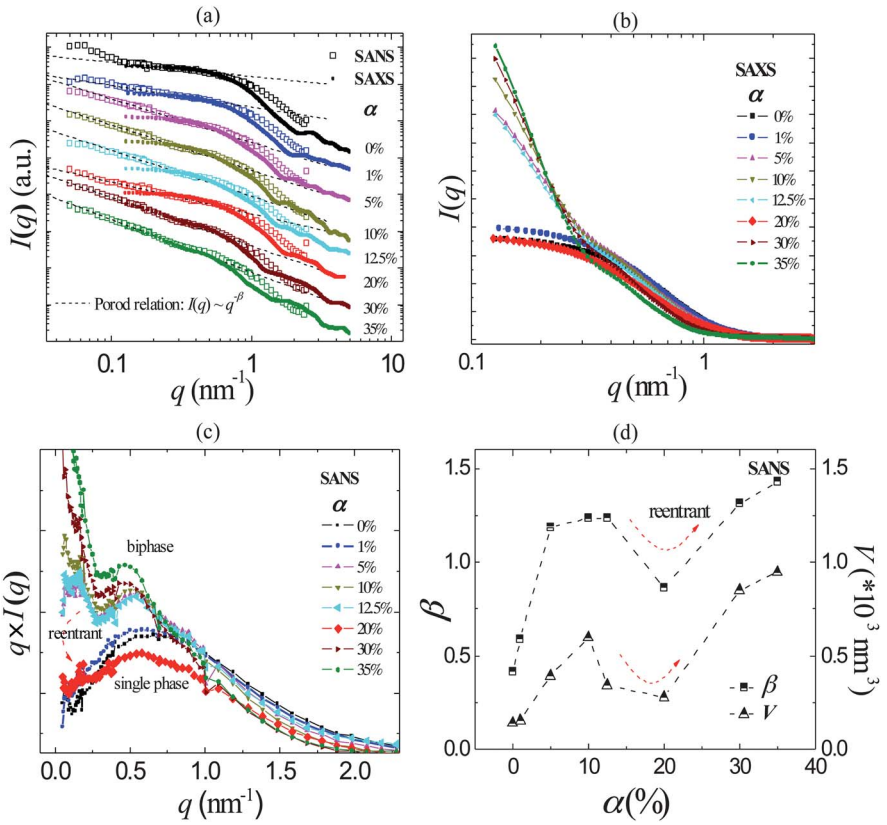

Fig. 1 Plots from SAXS/SANS at different α values in reciprocal space. (a) Logarithmic representation of $I(q)$ (SAXS: □, SANS: •) and Porod relation (---). (b) $I(q)$ from SAXS. (c) Holtzer plots from SANS. (d) $\beta \sim \alpha$ and $V \sim \alpha$ plots.

$\alpha = 20\%$, the $I(q)$ and the Holtzer plot seem to be similar to that when $\alpha = 0\%$ or $\alpha = 1\%$, respectively. It predicts, as expected, that the Quil A/Chol system reenters into a single phase. The onset of the reentrance can be attributed to the correlation attraction between almost neutral structures.[19] Thus, the electrostatic shielding of Quil A facilitates close monomer–monomer contacts. As a result, the systems collapse, drop out of equilibrium and are driven from a metastable state into an unstable spinodal region, and ultimately, form the small associates by the favorable entropic contribution. From this, we therefore arrive at an important point that the subtle balance between these microscopic forces, tuned by Chol, will lead to a controllable self-assembly and disassembly.

Further information about reentrant phase transition comes from the Porod relation:[20] $I(q) \sim q^{-\beta}$, where β is a fractal dimension exponent representing a particular shape of the complex. Its logarithmic representation is shown in Fig. 1a. From the derived $\beta \sim \alpha$ plot in Fig. 1d, the phase transition is precisely the same as that described in the Holtzer plots. $\beta = 0.41$ and $\beta = 1.43$ correspond to a sphere-like and a semi-flexible elongated rod-like morphology, respectively.[21] When $\alpha = 20\%$, $\beta = 0.86$ exhibits a critical boundary of the reentrant phase transition with a strong tendency of sphere-like reorganization that is more energetically favorable than short cylindrical one in an unstable phase. To support this result, one can also invoke the volume V of Quil A/Chol irrespective of its special shape. According to Porod (1951),[22] $V = 2\pi^2 I(q = 0)/Q$, here, the invariant Q is given by integral of the intensity $q^2 \times I(q)$ over reciprocal space. Change of V with α is also depicted in Fig. 1d. Evidently, a decrease of V characterizes the partial collapse or melting of associates, while an increase of V, in particular the re-increase starting from $\alpha = 20\%$, indicates the (retrieved) nucleation and growth. It is in agreement with the coarsening mechanisms of spinodal decomposition, according to which within the initial single phase a second phase spontaneously appears.[23] In addition, both $\beta \sim \alpha$ and $V \sim \alpha$ plots follow a non-linear relationship, which should point to a complex structural phase transition.

In contrast to the highly abstract nature of reciprocal space, an alternative way to straightforwardly analyze SAXS and SANS is in real space. In essence, each scattering function $I(q)$ in reciprocal space corresponds to a pair distance distribution function $p(r)$ in real space. The connection between them is described by indirect Fourier transformation introduced by Glatter,[22]

$$p(r) = \frac{r^2}{2\pi^2} \int_0^\infty I(q) \frac{\sin qr}{qr} q^2 \mathrm{d}q$$

where r denotes the distance of two scatters within a particle, and the maximum of r is defined as the particle size D when $p(r)$ drops to zero. The $p(r)$ distributions at different α values are plotted in Fig. 2.

The $p(r)$ in Fig. 2a and c, when $\alpha = 0\%$ or $\alpha = 1\%$, shows an approximately symmetric distribution around its single peak in the range $0 < r < 7$ nm. Such a distribution is usually taken as a sphere-like morphology of a micellar associate. A difference

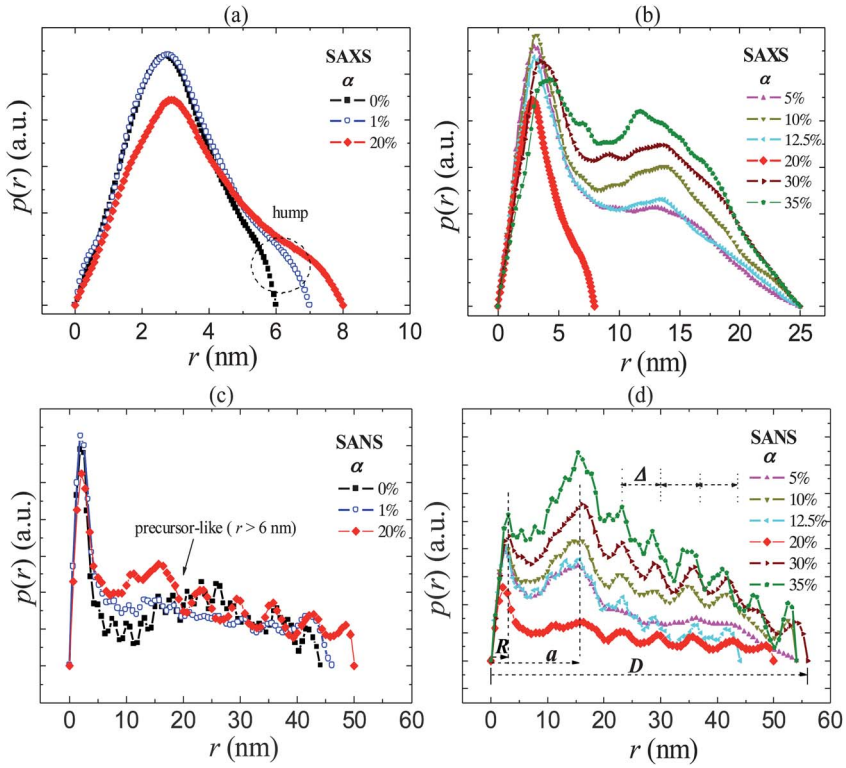

Fig. 2 Distance distribution function $p(r)$ from SAXS/SANS. (a and c) $p(r)$ distribution at lower α. (b and d) $p(r)$ distribution at higher α. For an experimental comparison, $p(r)$ distribution at $\alpha = 20\%$ is located in each of figures.

between them is that $p(r)$ from SANS exhibits a chain-like oscillatory distribution in a wider range of r from 6 to 50 nm, but in SAXS, no such effect is entailed, which, as already mentioned, is nothing but there is yet no effective local electronic density contrast.

In regard to the small humps when $\alpha = 1\%$, it indicates, in fact, that the sphere-like associate starts to distort even with slightly rising α, *i.e.* the micelles mostly remain sphere-like but also start to bring out locally disordered domains at low α. This means that, once depletion effects come into play, the volume of associate is re-adjusted, as shown in the $V \sim \alpha$ plot, so as to achieve the balance between associate–associate and monomer–monomer interactions.[23] More special is the chain-like oscillatory distribution, which offers more information about initial nucleation and can be identified with a precursor, highly viscoelastic non-equilibrium fluid, due to monomer correlation according to the monomer-addition model suggested by our previous work.[24] Moreover, the better matching for r between Fig. 2c and d also implies the presence of these precursors, which, in the sense of nucleation and initial microstructure formation in colloidal suspension, is one of the most fundamental aspects of phase transition and crystal growth and has a dramatic effect on the nucleation process such as epitaxial growth, ripening, size distribution of crystals and polymorphism.[25–27] This can be found out from Fig. 2b and d. The first peak is very similar to that in Fig. 2a and c, indicating the sphere-like morphology. The second peak in Fig. 2b, corresponding to that in Fig. 2d, and the multi-peak distribution in Fig. 2d highlight an elongated rod-like morphology grown out of precursors in the solution. And yet, one can, from two typical features of the multi-peak distribution, further ascertain this structure. First, the multi-peak distribution after the second peak is going to approximately linearly decrease as r increases. Second, the multi-peaks exhibit a periodicity, which arises from periodic local changes of deuterium-rich and -poor regimes organized by Chol-rich and -poor microdomains, and an almost symmetric distribution of each of the peaks. Clearly, it is not the case reflected by a perfectly rigid rod. Here, the elongated rod-like morphology can then be re-specified as a non-rigid helix-like morphology.[28] Of course, such re-specification is merely phenomenological. At a theoretical level, the helix-like structure growing on the chain-like precursor actually is a common effect of spinodal decomposition and heterogeneous nucleation, in which the structural interface is packed, tilted and bent, driven by the rigid hydrophobic property and self-perpetuation of the flip-flop motion of Chol, which should be comparable with the screw-dislocation-driven growth of nanowires and nanotubes.[29] From Fig. 2d it is convenient to get the sphere-like radius R, the radius a and pitch Δ of helix-like, and the spherohelix-like length D. For instance, in the case that $\alpha = 30\%$, $R \sim 3$ nm by the position of the first maximum in $p(r)$, $a \sim 16$ nm estimated by referring to the second maximum, $\Delta \sim 7$ nm and stands for an average distance between two neighbor maximums of $p(r)$ in the multi-peak distribution, and $D \sim 56$ nm. Notice that a given difference of D between Fig. 2b and d arises only out of the detection limit of SAXS and SANS. Such an idealized spherohelix-like associate is visualized in Fig. 3.

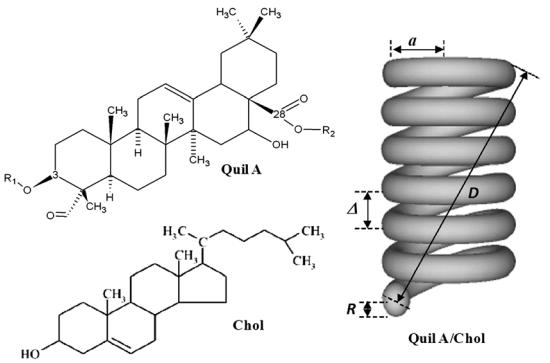

Fig. 3 Left: the general chemical structure of Quil A, where R_1 and R_2 are various sugar groups, and Chol. Right: sketch of an idealized spherohelix-like structure of Quil A/Chol.

More importantly, the reentrant phase transition, in $p(r)$ representation, has become clearer as shown in Fig. 2. When $\alpha = 20\%$, the first peak and the $p(r)$ distribution in the range of r from 8 to 50 nm nearly go back to that at $\alpha = 0\%$ or $\alpha = 1\%$. This fact especially shows that the latter reappears in the form of precursor-like and largely deviates from helix-like, and again supports the case of reentrant structural phase transition induced by Chol.

Finally, we have demonstrated the structural phase transition of the amphiphilic self-assembly brought about by Chol: sphere-like → spherohelix-like → sphere-like → spherohelix-like. Unlike in the standard sphero-cylinder model the reentrant phase transition has been missing, we underlined the dynamic process of reentrant phase transition. To summarize, this process can be represented as three stages. (i) Induction: formation of small sphere-like and chain-like precursors through monomer correlation. (ii) Conversion: distortion of the sphere-like and growth of helix-like precursors, in which the rigid Chol molecules steer the lipid packing, and drive the rod-like into helix-like by flip-flop motion. (iii) Decomposition: directly following collapse of the structures formed in (ii), they are rearranged into sphere-like and fluid-like precursors with an original helix-like signature. As such, the link between precursors and structural evolution, and the reentrant phase transition go far beyond the profile of the standard sphero-cylinder model. We hope that the results presented here would be helpful to rationalize the rich phase behavior exhibited by surfactant–cosurfactant systems, and to engineer complex nanoarchitectures with tunable size and shape and well-defined biological functions.

The authors would like to thank T. Paepenmüller for his technical contributions to the sample preparation.

References

1 V. J. Anderson and H. N. W. Lekkerkerker, *Nature*, 2002, **416**, 811–815.
2 S. May and A. Ben-Shaul, *J. Phys. Chem. B*, 2001, **105**, 630–640.

3 P. J. Flory, *J. Chem. Phys.*, 1941, **9**, 660; P. J. Flory, *J. Chem. Phys.*, 1942, **10**, 51–61.
4 M. L. Huggins, *J. Chem. Phys.*, 1941, **9**, 440.
5 I. G. Barr, A. Sjölander and J. C. Cox, *Adv. Drug Delivery Rev.*, 1998, **32**, 247–271.
6 T. Gilewski, G. Ragupathi, S. Bhuta, L. J. Williams, C. Musselli, X. F. Zhang, W. G. Bornmann, M. Spassova, K. P. Bencsath, K. S. Panageas, J. Chin, C. A. Hudis, L. Norton, A. N. Houghton, P. O. Livingston and S. J. Danishefsky, *Proc. Natl. Acad. Sci. U. S. A.*, 2001, **98**, 3270–3275.
7 S. H. E. Kaufmann and A. J. McMichael, *Nat. Med.*, 2005, **11**, S33–S44.
8 P. L. Yeagle, *Biochim. Biophys. Acta*, 1985, **822**, 267–287.
9 R. Rukmini, S. S. Rawat, S. C. Biswas and A. Chattopadhyay, *Biophys. J.*, 2001, **81**, 2122–2213.
10 M. S. Bretscher and S. Munro, *Science*, 1993, **261**, 1280–1281.
11 W. F. D. Bennett, J. L. MacCallum, M. J. Hinner, S. J. Marrink and D. P. Tieleman, *J. Am. Chem. Soc.*, 2009, **131**, 12714–12720.
12 F. Zhang, M. W. A. Skoda, R. M. J. Jacobs, S. Zorn, R. A. Martin, C. M. Martin, G. F. Clark and S. Weggler, *Phys. Rev. Lett.*, 2008, **101**, 148101.
13 L. A. Feigin, D. I. Svergun, *Structure analysis by small-angle-X-ray and neutron scattering*, ed. G. W. Taylor, Plenum press, New York and London, 1987.
14 G. D. Wignall, *J. Appl. Crystallogr.*, 1991, **24**, 479–484.
15 M. Schoeffel, N. Brodie-Linder, F. Audonnet and C. Alba-Simionesco, *J. Mater. Chem.*, 2012, **22**, 557–567.
16 N. E. Jacobsen, W. J. Fairbrother, C. R. Kensil, A. Lim, D. A. Wheeler and M. F. Powell, *Carbohydr. Res.*, 1996, **280**, 1–14.
17 R. Pool and P. G. Bolhuis, *Phys. Chem. Chem. Phys.*, 2010, **12**, 14789–14797.
18 M. H. J. Koch, P. Vachette and D. I. Svergun, *Q. Rev. Biophys.*, 2003, **36**, 147–227.
19 N. Grønbech-Jensen, J. R. Mashl, R. F. Bruinsma and W. M. Gelbart, *Phys. Rev. Lett.*, 1997, **78**, 2477.
20 B. Hammouda, *J. Appl. Crystallogr.*, 2010, **43**, 716–719.
21 *Neutrons, X-rays and Light: Scattering methods applied to soft condensed matter*, ed. P. Lindner and T. Zemb, North-Holland, Amsterdam, 2002.
22 O. Glatter and O. Kratky, *Small angle X-ray scattering*, Academic Press, New York, 1982.
23 A. Stradner, H. Sedgwick, F. Cardinaux, W. C. K. Poon, S. U. Egelhaaf and P. Schurtenberger, *Nature*, 2004, **432**, 492–495.
24 J. Liu, J. Rieger and K. Huber, *Langmuir*, 2008, **24**, 8262–8271.
25 A. Dey, P. H. H. Bomans, F. A. Müller, J. Will, P. M. Frederik, G. de With and N. A. J. M. Sommerdijk, *Nat. Mater.*, 2010, **9**, 1010–1014.
26 O. Galkin and P. G. Vekilov, *Proc. Natl. Acad. Sci. U. S. A.*, 2000, **97**, 6277–6281.
27 A. Cacciuto, S. Auer and D. Frenkel, *Nature*, 2004, **428**, 404–406.
28 C. D. Putnam, M. Hammel, G. L. Hura and J. A. Tainer, *Q. Rev. Biophys.*, 2007, **40**, 191–285.
29 J. Zhu, H. Peng, A. F. Marshall, D. M Barnett, W. D. Nix and Y. Cui, *Nat. Nanotechnol.*, 2008, **3**, 477–481.